227Ac Methods for Arctic Geotraces

Overview: The decay chain for 235U is shown in Fig. 1. This illustrates both how 227Ac is formed in the ocean, and also the decay scheme of its progeny that are used for its measurement. Maclane Pumps were deployed at various depths on the Geotraces cruise aboard the RV Healy (Cruise HLY 1502). Typically, a total of about 1500 L of water was pumped through two filter paths for collection of particulates, with about half going through a glass Fiber filter and the other half passing through a Supor filter. The effluent from the filters was combined and directed to a set of commercial acetate or acrylic cartridges that had been impregnated with MnO2. The approximate flow rate was 6 L/min during the pre-set pump time of 4 hours. Ac, Ra and Th in seawater were sorbed as water was pumped through them, although at this high flow rate, the sorption .efficiency was less than 100% for each of these isotopes. Presumably, 231Pa, the 227Ac parent was also sorbed because it is very particle reactive. Analyses of Ra and Th on these cartridges have been made by collaborating groups (M. Charette at WHOI and W. Moore at U. So. Carolina).

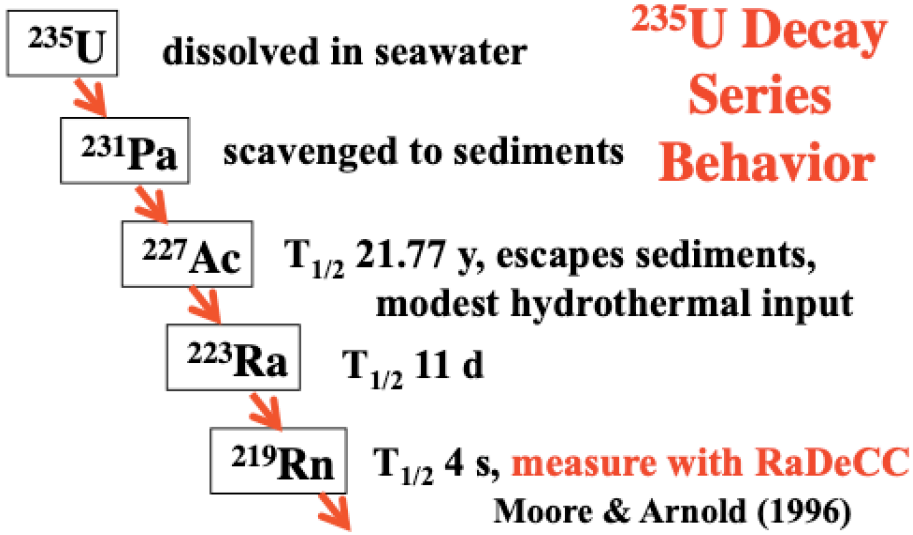

Fig. 1. 235U decay chain showing positions of 227Ac and the 219Rn progeny measured with Radecc. Comments about the behavior of each isotope in the chain are at right. Several intermediates in the series are not shown.

Two cartridges were used in series (A and B), allowing the 227Ac extraction efficiency from seawater at high pump rates to be calculated (see below). After extracting 227Ac in the field, it was be analyzed in the lab. A stream of He passed through these fibers to transport the 219Rn progeny from 227Ac decay into a Radecc counter (Moore and Arnold, 1996). Radecc has circuitry that can distinguish decays of 219Rn, 220RRn and 222Rn by opening windows following detection of an alpha decay. If a second decay is observed in these windows from a short-lived Po daughter, its arrival time can be used to distinguish which Rn may have produced the initial signal.

Considerable time was spent on confirming the accuracy of the Radecc method, including preparation of new standards for 227Ac and evaluating standard stability, effects of geometry, flow rate used for analysis, and "crosstalk" that has been observed for Radecc channels measuring 219Rn and 220Rn (descendants of 227Ac and 228Ra). Sections below show details of data reduction and calibration.

RaDeCC Data Reduction: The instrument opens two windows when an alpha decay is detected. The first (219 window) spans 0.01 to 5.60 ms and the second (220 window) spans 5.61 to 600 ms. Any subsequent decays occurring in each window are recorded. Decays of 219Rn lead to decays of 215Po that primarily occur in the 219 window and decays of 220Rn lead to decays of 216Po that primarily occur in the 220 window. The total record for events observed in successive 10 minute intervals are stored in a text file. A Matlab program was written to read these files, correct the values in each window for random decays of other isotopes, and for decays of 219 that occur in the 220 window plus decays of 220 that decay in the 219 window. The program plots the corrected activity vs. time. Random events resulting in chance coincidence in each window build up over time, and when these become large enough to dominate the window signal, the count is terminated. Water evaporating from the wet sample can condense in the detector and reduce efficiency during the count. If air leaks into the helium counting matrix, efficiency can also drop. These decreases in efficiency can be evaluated from the window signals vs. time, and the count is terminated when this poses a problem. For the Arctic samples, each count was 120 to 350 minutes, depending on the behavior observed. Anomalous signals indicating counter noise can also be detected and removed (rare).

Computations have been described by Moore and Arnold (1996), although two corrections were made for this work. For each channel:
$cc\# = R^2 t_g/(1-Rt_g)$
where cc# is chance counts for the window # and t_g, is the window open interval;
R = random single events = BC - AC
where BC = total count rate and AC = sum of 219 and 220 window count rates;
$cc219 = (t1/tg)\ R^2(tg)/(1-R*tg)$
$cc220 = (t2/tg)\ R^2(tg)/(1-R*tg)$
where t1 and t2 are the duration of the 219 and 220 windows and tg is t1+t2. This corrects the algorithm with the addition of the first term on the right of the cc219 and cc220 expressions above. It makes little difference for low activity samples, but becomes significant at high count rates.

The second change was to solve simultaneous equations to correct for 219 in the 220 window and 220 in the 219 window from the signals after correction for chance counts:
Final 219 cpm = corr219 - 0.0288*(corr220)
Final 220 cpm = corr220 - 0.1279*(corr219)
With the constants in the equations above determined from the window durations and the Po daughter decay constants.

The matlab routine calculates uncertainties as the standard deviation of the means of the 10 minute counting interval lines.

Geometry and Standard Calibration: Two types of sample geometry have been used extensively by the community. The traditional one was developed by Moore (1976) and uses acrylic fibers coated with MnO2, housed in an acrylic tube about 200 cc in volume (identified here as MF geometry). The second type (used in Geotraces sampling by many groups) uses a commercial water filter coated with MnO2, housed in a commercial filter holder (~450 cc, identified here as CC geometry). A standard solution obtained by our collaborators at WHOI was obtained from Eckert and Ziegler, diluted, and sent to USC. This solution was used to prepare standards in the Geotraces CC geometry by adding an aliquot of spike to about 1 L of Ra-free seawater (prepared by passing through Mn-fibers in a MF cartridge). The spiked seawater was then passed through a cartridge 5 times at about 1 L/min to ensure all Ac was sorbed. The residual seawater was later checked for 223Ra activity to be sure no Ac had remained in the solution or on the walls of the bottle. No activity was found. Multiple standards were prepared. In addition, standards were prepared on acrylic fibers (MF geometry). One historical standard prepared from a calibrated solution of dissolved urananite (std 27) has been in use in our lab and was run regularly during the analysis of Arctic samples to ascertain any deterioration of detectors during this time. The relative efficiency of 5 of our 6 detectors remained constant while Arctic samples were being analyzed. The 6th channel showed a near linear drop in efficiency with time, apparently due to water progressive water damage. Samples run on this channel lost several grams of water in each run, likely causing deterioration. Counting efficiency for std 27 vs. time was fit with a linear function to determine the relative change in efficiency for this counter.

Radon Release Factor: We had previously found that Pacific samples in the CC geometry released 219Rn about 30% more slowly than the MF geometry, resulting in lowered counting efficiency. Using the newly obtained standard solution containing 227Ac, we confirmed that previous work we had done in the South Pacific was correctly standardized. We also confirmed that results of Scholten et al. (2010) showing that the 219Rn counting efficiency for standards mounted in the MF geometry decreased by 5-20% over several months after preparation. The likely cause of this decrease is that alpha recoil of 227Ac descendant 223Ra buries it deeply in these fibers that its 219Rn progeny do not escape as efficiently as 219Rn progeny from 223Ra initially sorbed on the fiber. This is not a problem for 220Rn, as it has a half-life that is ~25x longer than 219Rn, and it escapes from the fiber very efficiently. The standard efficiency decrease with time was not found to be a problem for standards in CC geometry, as we have found these to be very stable for several years. The release factor of 0.70 at our normal flow rate, previously found, was confirmed using standards in the CC geometry.

Flow Rate Effects for Radecc: The CC geometry has been found to be much more sensitive to flow rate than the MF geometry (Fig. 2). It was critical for the CC geometry to keep flow rate in the normal range to obtain consistent results.

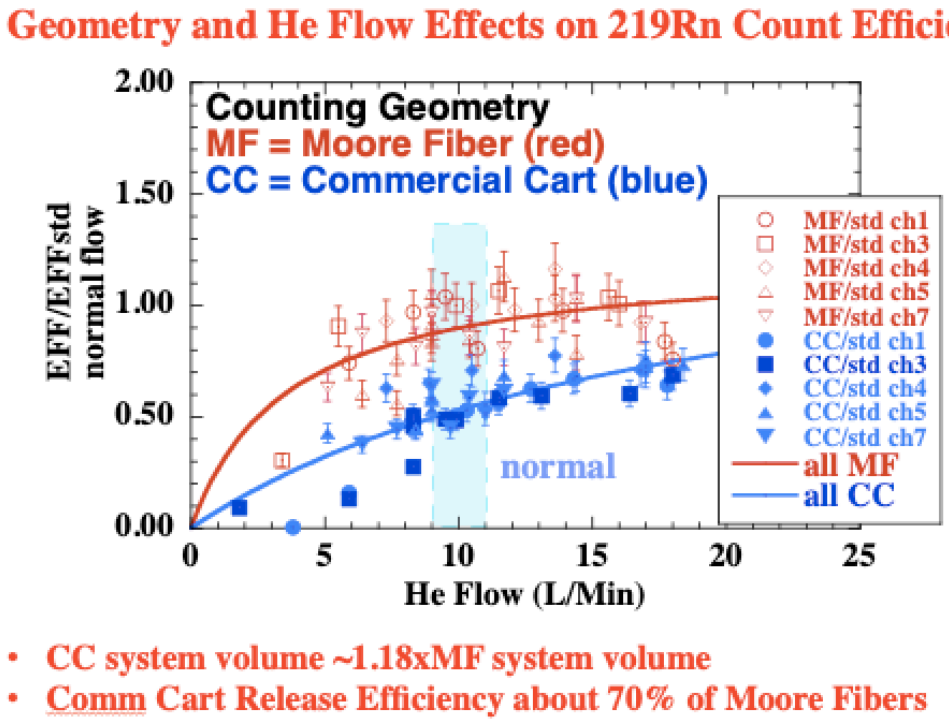

Fig. 2. Effect of flow rate on 219Rn detection with Radecc. The CC geometry has a much lower counting efficiency than MF geometry. This reflects the volume of the counting system (1.18x larger with CC geometry) and also a lower efficiency (~0.70) of 219Rn release from the coated fibers in CC geometry. The difference in flow rate dependence of the two geometries indicates the release efficiency factor depends on flow rate. The shaded blue region is our selected operation condition.

Channel Crosstalk: Signals in the 219Rn channel are created by high activity in the 220Rn channel (Fig. 3). The effect remains after correcting the 219 counts for contributions from decay of the 216Po that is expected in the 219 window. This was particularly a problem for shallow water Arctic samples that contained very high activities of 228Ra and low activities of 227Ac, as the correction introduced large uncertainties. Scholten et al. (2010) had previously noted this feature. We have confirmed it, and found it seems to be independent of channel identity. There does not seem to be an effect of high 219Rn on the 220Rn channel. The cause of the signal is unidentified. The following algorithm was used to correct 219 cpm for 220 cpm:

220 cpm	Crosstalk in 219 cpm
0-2	no correction
2-6.6	0.0358*(220cpm) - 0.012
>6.6	0.06433*(220cpm-6) + 0.0358

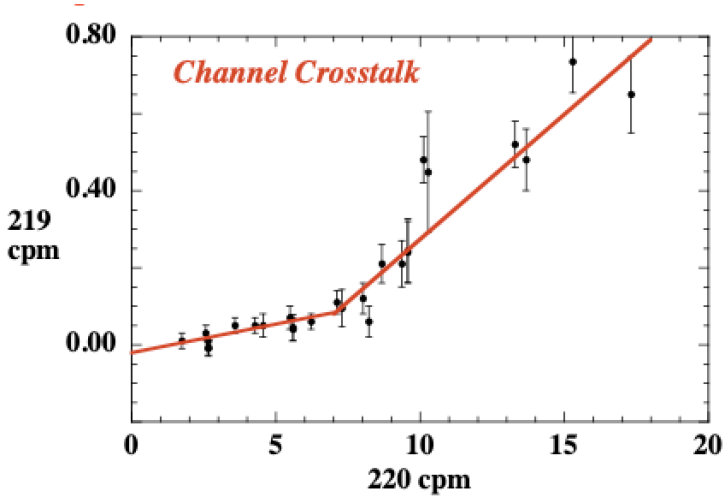

Fig. 3. Signals of 219Rn observed when a pure source of high 220Rn is introduced into Radecc. The normal corrections for chance coincidence have been made, and this is the residual signal. Note the non-linearity. The cause has not been identified.

Cartridge Sorption Efficiency: When cartridges are in series, the sorption efficiency can be determined from the ratio of activities on the two cartridges, A_B/A_A:

$E = 1 - A_B/A_A$

Large uncertainties exist for the ratio at different stations, as activities were quite low. Consequently, a median value was found for all samples where the uncertainty in the ratio was less than ±0.4, with the median for this group of 0.62. With two cartridges in series, this should capture the fraction $2*E = E^2 = 0.856$ of the Ac. Consequently, total Ac for the sample was computed (method a) as $Ac = (A_A + A_B)/(0.856)$. If only one cartridge was deployed (24 samples), method b was used as $Ac = A_A/(0.62)$. In one case, the A cartridge was not analyzed, and method c was used, $Ac = A_B/(E*(1-E))$ In a one case, the ratio of the two cartridges exceeded 1.5, indicating a likely bypass of the first cartridge or perhaps a poor MnO2 coating. In this case, method d was used where $Ac = A_A + (A_B)/(0.62)$. Comparison of the CC cartridge efficiencies for both Th and Ac indicated the two elements have comparable sorption efficiency (Fig. 4). Also, sorption efficiency for Arctic samples was very close to that for the South Pacific Samples (0.65) collected in 2013 and a value of 0.65 found by Geibert et al. (2002) in the Antarctic. The variability of efficiency among cartridges is difficult to evaluate because of the poor counting statistics. Because the variation in E is comparable to the ~30% uncertainty in counting statistics, the uncertainty in efficiency among cartridges is estimated at 10%. A Monte Carlo analysis of the effect on Ac uncertainty was run and showed that this should introduce only about 3% uncertainty in Ac determination. When method b is used, the uncertainty contribution rises to 10%.

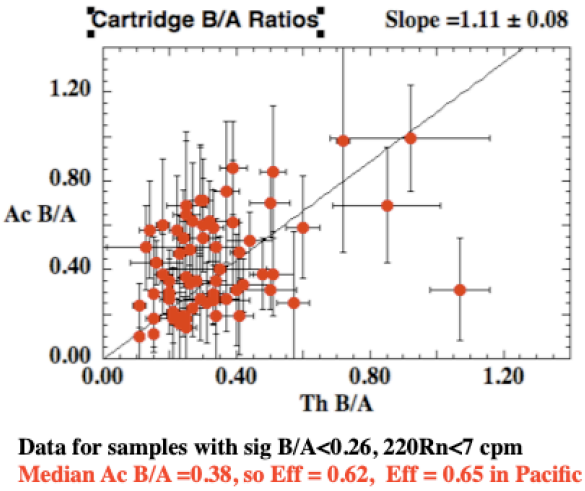

Fig. 4. Sorption efficiency for Ac vs. Th. The Sorption Efficiency for a pair of cartridges is $E = 1 - A_B/A_A$, where A_A and A_B are activities for cartridges in series.

227Ac Concentration and Uncertainty Calculations: Typically, each cartridge was counted 2-3 times using different counters. Results were averaged and the standard deviation of the mean (sdom) was calculated. The uncertainty was also calculated from the uncertainties of each measurement. These were usually quite close to the sdom, and the larger of the two uncertainties was assumed. Contributions of uncertainties from crosstalk corrections and the modest uncertainty from cartridge efficiency were included by error propagation expressions. Total Ac and its uncertainty were divided by the water volume pumped to find concentration.

Excess 227Ac: Analyses of the 227Ac parent 231Pa were done on Niskin water samples that were usually a few meters vertically from the pumps. These were performed by collaborating groups (personal communication from R. Anderson of LDEO and L. Edwards of U. Minnesota). Their results were subtracted from total Ac to calculate excess 227Ac. In a few cases, it was necessary to interpolate over larger distances, but the uncertainty from this is expected to be small. No effect on Ac uncertainties is expected, as the 231Pa measurements have a precision of only a few percent. Most samples that were not near the surface or bottom have negligible excess 227Ac in comparison to the uncertainties indicating the 227Ac is accurately calibrated (Fig. 5).

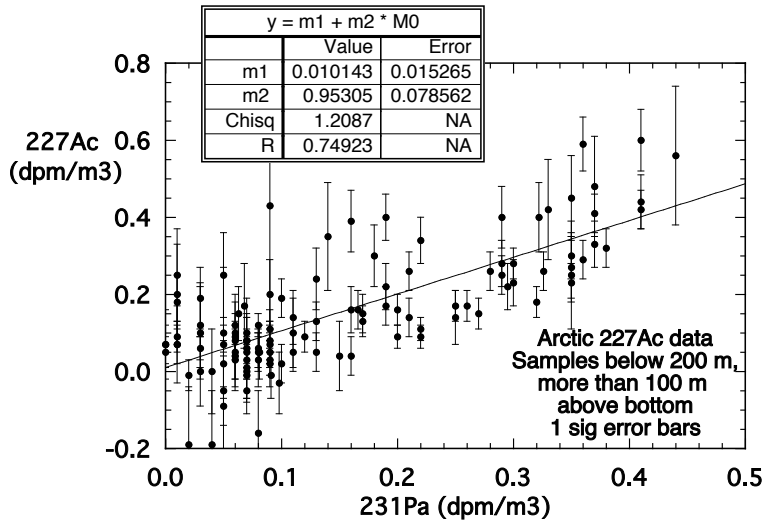

Fig. 5. 227Ac vs 231Pa for samples below 200 m depth and more than 100 m above bottom. Error bars are ± 1 sdom for 227Ac and those for 231Pa are negligible. A regression has an uncertainty of 0.01±0.02 and a slope of 0.95±0.08, indicating that the two isotopes are in secular equilibrium for the water column and the results for the two parameters are well calibrated. About 2/3 of the data points should have error bars (±1 sdom) that intersect the regression, approximately what is observed.

References

Geibert, W., M.M. Rutgers van der Loeff, C. Hanfland, H.-J. Dauelsberg (2002) Actinium-227 as a deep-sea tracer: sources, distribution and applications, Earth. Planet. Sci. Lett. 198, 147-165.

Moore, W.S. (1976) Sampling radium-228 in the deep ocean, Deep-Sea Res. 23, 647-651.

Moore, W.S., and R. Arnold (1996) Measurement of 223Ra and 224Ra in coastal waters using a delayed coincidence counter, J. Geophys. Res. 101, 1321-1329.

Scholten, J.C., M.K. Pham, O. Blinova, M.A. Charette, H. Dulaiova, and M. Eriksson (2010), Preparation of Mn-fiber standards for the efficiency calibration of the delayed coincidence counting system (RaDeCC), Mar. Chem. 121, 206-214. doi: 10.1016/j.marchem.2010.04.09

Related Data Sets

Charette, M., https://www.bco-dmo.org/project/718522

Anderson, R., M. Fleisher and L. Edwards, 231Pa on GN01. Personal communication.